Artificial intelligence-enabled quantitative coronary plaque and hemodynamic analysis for predicting acute coronary syndrome

Koo, B.K.; Yang, S.; Jung, J.W.; Zhang, J.; Lee, K.; Hwang, D.; ... ; Narula, J.

JACC: CARDIOVASCULAR IMAGING VOL. 17, NO. 9, 2024

PUBLISHED BY ELSEVIER

ORIGINAL RESEARCH

Artificial Intelligence–Enabled Quantitative Coronary Plaque and Hemodynamic Analysis for Predicting Acute Coronary Syndrome

Bon-Kwon Koo, MD, PhD,[a,*] Seokhun Yang, MD,[a,*] Jae Wook Jung, MD,[a] Jinlong Zhang, MD, PhD,[b] Keehwan Lee, MD,[a] Doyeon Hwang, MD,[a] Kyu-Sun Lee, MD, PhD,[c] Joon-Hyung Doh, MD, PhD,[d] Chang-Wook Nam, MD, PhD,[e] Tae Hyun Kim, MD,[f] Eun-Seok Shin, MD, PhD,[g] Eun Ju Chun, MD, PhD,[h] Su-Yeon Choi, MD, PhD,[i] Hyun Kuk Kim, MD, PhD,[j] Young Joon Hong, MD, PhD,[k] Hun-Jun Park, MD, PhD,[l] Song-Yi Kim, MD,[m] Mirza Husic, MD, PhD,[n] Jess Lambrechtsen, MD, PhD,[n] Jesper M. Jensen, MD, PhD,[o] Bjarne L. Nørgaard, MD, PhD,[o] Daniele Andreini, MD, PhD,[p,q] Pal Maurovich-Horvat, MD, PhD,[r] Bela Merkely, MD, PhD,[s] Martin Penicka, MD, PhD,[t] Bernard de Bruyne, MD, PhD,[t] Abdul Ihdayhid, MD, PhD,[u] Brian Ko, MD, PhD,[u] Georgios Tzimas, MD,[v] Jonathon Leipsic, MD, PhD,[v] Javier Sanz, MD,[w] Mark G. Rabbat, MD,[x] Farhan Katchi, MD,[y] Moneal Shah, MD,[z] Nobuhiro Tanaka, MD, PhD,[aa] Ryo Nakazato, MD, PhD,[bb] Taku Asano, MD, PhD,[bb] Mitsuyasu Terashima, MD, PhD,[cc] Hiroaki Takashima, MD, PhD,[dd] Tetsuya Amano, MD, PhD,[dd] Yoshihiro Sobue, MD, PhD,[ee] Hitoshi Matsuo, MD, PhD,[ee] Hiromasa Otake, MD, PhD,[ff] Takashi Kubo, MD, PhD,[aa] Masahiro Takahata, MD, PhD,[gg] Takashi Akasaka, MD, PhD,[gg] Teruhito Kido, MD, PhD,[hh] Teruhito Mochizuki, MD, PhD,[hh] Hiroyoshi Yokoi, MD, PhD,[ii] Taichi Okonogi, MD,[jj] Tomohiro Kawasaki, MD, PhD,[jj] Koichi Nakao, MD, PhD,[kk] Tomohiro Sakamoto, MD, PhD,[kk] Taishi Yonetsu, MD, PhD,[ll] Tsunekazu Kakuta, MD, PhD,[mm] Yohei Yamauchi, MD, PhD,[nn] Jeroen J. Bax, MD, PhD,[oo] Leslee J. Shaw, PhD,[w] Peter H. Stone, MD,[pp] Jagat Narula, MD, PhD[qq]

ABSTRACT

BACKGROUND A lesion-level risk prediction for acute coronary syndrome (ACS) needs better characterization.

OBJECTIVES This study sought to investigate the additive value of artificial intelligence–enabled quantitative coronary plaque and hemodynamic analysis (AI-QCPHA).

METHODS Among ACS patients who underwent coronary computed tomography angiography (CTA) from 1 month to 3 years before the ACS event, culprit and nonculprit lesions on coronary CTA were adjudicated based on invasive coronary angiography. The primary endpoint was the predictability of the risk models for ACS culprit lesions. The reference model included the Coronary Artery Disease Reporting and Data System, a standardized classification for stenosis severity, and high-risk plaque, defined as lesions with ≥2 adverse plaque characteristics. The new prediction model was the reference model plus AI-QCPHA features, selected by hierarchical clustering and information gain in the derivation cohort. The model performance was assessed in the validation cohort.

RESULTS Among 351 patients (age: 65.9 ± 11.7 years) with 2,088 nonculprit and 363 culprit lesions, the median interval from coronary CTA to ACS event was 375 days (Q1-Q3: 95-645 days), and 223 patients (63.5%) presented with myocardial infarction. In the derivation cohort (n = 243), the best AI-QCPHA features were fractional flow reserve across the lesion, plaque burden, total plaque volume, low-attenuation plaque volume, and averaged percent total myocardial blood flow. The addition of AI-QCPHA features showed higher predictability than the reference model in the validation cohort (n = 108) (AUC: 0.84 vs 0.78; $P < 0.001$). The additive value of AI-QCPHA features was consistent across different timepoints from coronary CTA.

CONCLUSIONS AI-enabled plaque and hemodynamic quantification enhanced the predictability for ACS culprit lesions over the conventional coronary CTA analysis. (Exploring the Mechanism of Plaque Rupture in Acute Coronary Syndrome Using Coronary Computed Tomography Angiography and Computational Fluid Dynamics II [EMERALD-II]; NCT03591328) (JACC Cardiovasc Imaging. 2024;17:1062–1076) © 2024 by the American College of Cardiology Foundation.

ISSN 1936-878X/$36.00 https://doi.org/10.1016/j.jcmg.2024.03.015

Acute coronary syndrome (ACS) remains the leading cause of mortality worldwide.[1,2] Three-fourths of patients with myocardial infarction (MI) present as new coronary artery events,[3] and MI precursors can be related to nonobstructive stenoses.[4,5] Accordingly, risk evaluation for future ACS events is required in the upfront diagnostic stage before fatal coronary events or severe obstructive coronary stenosis.

Coronary computed tomography angiography (CTA) is the established noninvasive imaging modality to diagnose coronary artery disease (CAD).[6,7] The recent ESC (European Society of Cardiology) and ACC (American College of Cardiology)/AHA (American Heart Association) guidelines recommend the use of coronary CTA as a first-line test in patients with suspected CAD because of its excellent negative predictive value, which enables exclusion of CAD.[8,9] In addition to assessment of stenosis severity, coronary CTA can also identify adverse plaque characteristics (APCs) associated with an increased risk of ACS,[10] and the standard coronary CTA interpretation criteria encompass both stenosis severity and APCs.[11] However, their low positive predictive value for treatment decision making in clinical practice necessitates the use of an additional metric to enhance prediction of future ACS events.[12]

The biomechanical substrate of atherosclerotic coronary lesions leading to ACS comprises complex interactions between plaque composition and the hemodynamic environment surrounding the plaque. Therefore, combined plaque and hemodynamic analysis can enhance the identification of characteristics that may lead to ACS.[13-15] Nonetheless, the plaque and hemodynamic analyses have been operator dependent, and a comprehensive risk model based on artificial intelligence (AI)-enabled quantitative analysis, which incorporates plaque and hemodynamic characteristics, has yet to be fully established. In this regard, the current study aims to identify the plaque and hemodynamic features for ACS prediction using AI-based analysis and investigate their additive value to the stenosis severity and APCs and explore their potential implications for selecting appropriate treatment strategies.

METHODS

STUDY POPULATION. EMERALD-II (Exploring the Mechanism of Plaque Rupture in Acute Coronary Syndrome Using Coronary Computed Tomography Angiography and Computational Fluid Dynamics II) recruited ACS patients who underwent coronary CTA 1 month to 3 years before the ACS from 9 countries (United States, Canada, Denmark, Italy, Hungary, Belgium, Australia, Japan, and South Korea). The definition of MI followed the universal criteria,[16] whereas unstable angina was defined as the presence of culprit lesions with

ABBREVIATIONS AND ACRONYMS

ACS = acute coronary syndrome

AI-QCPHA = artificial intelligence–enabled quantitative coronary plaque and hemodynamic analysis

APC = adverse plaque characteristic

APS = axial plaque stress

CAD = coronary artery disease

CTA = computed tomography angiography

FFR_{CT} = fractional flow reserve derived from coronary computed tomography angiography

HRP = high-risk plaque

ICA = invasive coronary angiography

LAPV = low-attenuation plaque volume

MBF = myocardial blood flow

MI = myocardial infarction

NCPV = noncalcified plaque volume

TPV = total plaque volume

WSS = wall shear stress

From the [a]Department of Internal Medicine and Cardiovascular Center, Seoul National University Hospital, Seoul National University of College of Medicine, Seoul, South Korea; [b]Department of Cardiology, The Second Affiliated Hospital, School of Medicine, Zhejiang University, Hangzhou, China; [c]Department of Cardiology, Eulji University Medical Center, Daejeon, South Korea; [d]Department of Medicine, Inje University Ilsan Paik Hospital, Goyang, South Korea; [e]Department of Medicine, Keimyung University Dongsan Medical Center, Daegu, South Korea; [f]Department of Cardiology, Ulsan Medical Center, Ulsan, South Korea; [g]Department of Cardiology, Ulsan University Hospital, University of Ulsan College of Medicine, Ulsan, South Korea; [h]Department of Radiology, Seoul National University Bundang Hospital, Seongnam, South Korea; [i]Department of Internal Medicine, Seoul National University Hospital Healthcare System Gangnam Center, Seoul, South Korea; [j]Department of Internal Medicine and Cardiovascular Center, Chosun University Hospital, University of Chosun College of Medicine, Gwangju, South Korea; [k]Department of Cardiology, Chonnam National University Hospital, Gwangju, South Korea; [l]Division of Cardiology, Department of Internal Medicine, Seoul St. Mary's Hospital, The Catholic University of Korea, Seoul, South Korea; [m]Division of Cardiology, Department of Internal Medicine, Jeju National University Hospital, Jeju, South Korea; [n]Department of Cardiology, Odense University Hospital, Svendborg, Denmark; [o]Department of Cardiology, Aarhus University Hospital, Aarhus, Denmark; [p]Centro Cardiologico Manzano, Istituti di Ricovero e Cura a Carattere Scientifico, Milan, Italy; [q]Department of Biomedical and Clinical Sciences, University of Milan, Milan, Italy; [r]Department of Radiology, Medical Imaging Centre, Semmelweis University, Budapest, Hungary; [s]The Heart and Vascular Center, Semmelweis University, Budapest, Hungary; [t]Cardiovascular Center Aalst, Onze Lieve Vrouwziekenhuis-Clinic, Aalst, Belgium; [u]Monash Cardiovascular Research Centre, Monash University and Monash Heart, Monash Health, Clayton, Victoria, Australia; [v]Department of Medicine and Radiology, University of British Columbia, Vancouver, British Columbia, Canada; [w]Cardiovascular Institute, Icahn School of Medicine at Mount Sinai, New York, New York, USA; [x]Division of Cardiology, Loyola University Chicago, Chicago, Illinois, USA; [y]Department of Cardiology, Washington University School of Medicine in St. Louis, Missouri, USA; [z]Department of Cardiology, Allegheny General Hospital, Pittsburgh, Pennsylvania, USA; [aa]Department of Cardiology, Tokyo Medical University Hachioji Medical Center, Tokyo, Japan; [bb]Cardiovascular Center, St Luke's International Hospital, Tokyo, Japan; [cc]Department of Cardiovascular Medicine, Toyohashi Heart Center, Aichi, Japan; [dd]Department of Cardiology, Aichi Medical University,

JACC: CARDIOVASCULAR IMAGING, VOL. 17, NO. 9, 2024
SEPTEMBER 2024:1062–1076

suspected plaque rupture or thrombus or with angiographic stenosis of ≥90%. Patients with the following characteristics were excluded: 1) those with no clear evidence of culprit lesion; 2) those with previous stent implantation in 2 or more coronary arteries (vessel territories) before coronary CTA or revascularization between coronary CTA and the ACS event; 3) those with the ACS culprit lesion in a previously stented segment; 4) those with secondary ACS or history of coronary artery bypass graft surgery; and 5) those with poor-quality coronary CTA not suitable for quantitative plaque and hemodynamic analysis. The study protocol was approved by the Institutional Review Board of each site and was performed in accordance with the Declaration of Helsinki (NCT03591328).

STUDY DESIGN. The detailed study design is presented in Supplemental Figure 1. Patients undergoing invasive coronary angiography (ICA) following ACS were identified by searching the database of participating centers, and those who had undergone coronary CTA from 1 month to 3 years before the ACS event and met the inclusion criteria were enrolled in the study. Clinical characteristics, coronary CTA, and ICA images were collected and analyzed by independent core laboratories. Coronary CTA images were sent to 2 independent coronary CTA core laboratories for quantitative plaque and hemodynamic analysis (HeartFlow Inc) and for conventional coronary CTA analysis according to the standard coronary CTA interpretation criteria[11] (University of British Columbia). ICA images were sent to the angiographic core laboratory (Samsung Medical Center) blinded to patient characteristics and coronary CTA findings to define the ACS culprit lesion. For each patient, all lesions were matched between coronary CTA and ICA images, and subsequently, culprit and nonculprit lesions on coronary CTA were labeled. The culprit lesions were defined as cases and the nonculprit lesions of ACS as internal controls (Supplemental Figure 1). The enrolled patients were assigned to either the derivation or validation cohort in a blinded manner, with matching based on age, sex, diabetes, diagnosis, and the time interval between coronary CTA and the ACS event. The division of the total population into derivation and validation cohorts was based on the sample size calculations required for each cohort, detailed in the Supplemental Methods. The Seoul National University Hospital Clinical Trial Center acted as a dedicated affiliated research coordinator. Clinical data were collected using a computerized database and were reviewed by an independent trial monitor.

AI-ENABLED QUANTITATIVE CORONARY PLAQUE AND HEMODYNAMIC ANALYSES. The details regarding the computed tomography scanner used for the study population are presented in Supplemental Table 1. The image quality of coronary CTA was reviewed by the core laboratory. Among vessels with a reference diameter of >2 mm, lesions with a percent diameter stenosis of >20% in the main epicardial vessels or >30% in the side branches and/or plaque burden of >50% were submitted for artificial intelligence–enabled quantitative plaque and hemodynamic analysis (AI-QCPHA).[17] The detailed AI-QCPHA is described in the Supplemental Methods. Hemodynamic characteristics comprising averaged wall shear stress (WSS), peak WSS, averaged axial plaque stress (APS), peak APS, change in fractional flow reserve derived from coronary CTA (FFR_{CT}) across the lesion (ΔFFR_{CT}), peak FFR_{CT} gradient, averaged percent total myocardial blood flow (MBF), peak percent total MBF, averaged percent left ventricular MBF, and peak percent left ventricular MBF. Quantitative plaque characteristics included plaque burden (a cross-sectional plaque area/vessel area at the minimum lumen area site); total plaque volume (TPV); noncalcified plaque volume (NCPV) (plaque composition

Nagakute, Japan; [ee]Department of Cardiovascular Medicine, Gifu Heart Center, Gifu, Japan; [ff]Division of Cardiovascular Medicine, Department of Internal Medicine, Kobe University Graduate School of Medicine, Kobe, Japan; [gg]Department of Cardiovascular Medicine, Wakayama Medical University, Wakayama, Japan; [hh]Department of Radiology, Ehime University Graduate School of Medicine, Ehime, Japan; [ii]Cardiovascular Center, Fukuoka Sanno Hospital, Fukuoka, Japan; [jj]Cardiovascular Center, Shin-Koga Hospital, Kurume, Japan; [kk]Division of Cardiology, Saiseikai Kumamoto Hospital Cardiovascular Center, Kumamoto, Japan; [ll]Department of Cardiovascular Medicine, Tokyo Medical and Dental University, Tokyo, Japan; [mm]Division of Cardiovascular Medicine, Tsuchiura Kyodo General Hospital, Ibaraki, Japan; [nn]Department of Cardiology, Osaka Medical and Pharmaceutical University, Takatsuki, Japan; [oo]Department of Cardiology, Heart Lung Centre, Leiden University Medical Centre, Leiden, the Netherlands; [pp]Division of Cardiovascular Medicine, Brigham and Women's Hospital, Harvard Medical School, Boston, Massachusetts, USA; and the [qq]McGovern Medical School, University of Texas Health Sciences Center, Houston, Texas, USA.
*Drs Koo and Yang contributed equally to this work.

Maros Ferencik, MD, served as Guest Editor for this paper.
The authors attest they are in compliance with human studies committees and animal welfare regulations of the authors' institutions and Food and Drug Administration guidelines, including patient consent where appropriate. For more information, visit the Author Center.

Manuscript received October 24, 2023; revised manuscript received March 13, 2024, accepted March 20, 2024.

TABLE 1 Baseline Patient Characteristics

	Total Patients (N = 351)	Derivation Cohort (n = 243)	Validation Cohort (n = 108)	*P* Value
Age, y	65.9 ± 11.7	65.8 ± 11.8	66.0 ± 11.7	0.860
Male	261 (74.4)	182 (74.9)	79 (73.1)	0.831
Diagnosis				0.919
Myocardial infarction	223 (63.5)	156 (64.2)	67 (62.0)	
NSTEMI	128 (36.5)	90 (37.0)	38 (35.2)	
STEMI	95 (27.1)	66 (27.2)	29 (26.9)	
Unstable angina	128 (36.5)	87 (35.8)	41 (38.0)	0.789
Diabetes	116 (33.0)	82 (33.7)	34 (31.5)	0.769
Hypertension	258 (73.5)	179 (73.7)	79 (73.1)	>0.999
Hyperlipidemia	218 (62.1)	152 (62.6)	66 (61.1)	0.891
Current smoker	84 (23.9)	61 (25.1)	23 (21.3)	0.525
Time to event from coronary CTA to ACS event, d	375.0 (95.0-644.5)	381.0 (97.0-640.5)	361.5 (94.5-662.0)	0.967
Medications at the time of coronary CTA				
Aspirin or $P2Y_{12}$ inhibitor	155 (44.3)	111 (45.9)	44 (40.7)	0.438
ACEI/ARB	127 (36.3)	86 (35.5)	41 (38.0)	0.752
Beta-blocker	82 (23.4)	57 (23.6)	25 (23.1)	>0.999
Calcium channel blocker	89 (25.4)	63 (26.0)	26 (24.1)	0.798
Statin	134 (38.3)	93 (38.4)	41 (38.0)	>0.999

Values are n (%), mean ± SD, or median (Q1-Q3). Diabetes was defined as fasting plasma glucose level of ≥126 mg/dL, glycated hemoglobin of ≥6.5%, or treatment with any antidiabetic drugs. Hyperlipidemia was defined as triglycerides of ≥200 mg/dL, total cholesterol of ≥240 mg/dL, low-density lipoprotein cholesterol of ≥160 mg/dL, high-density lipoprotein cholesterol of <40 mg/dL, or treatment with any lipid-lowering medications.

ACEI = angiotensin-converting enzyme inhibitor; ACS = acute coronary syndrome; ARB = angiotensin receptor blocker; CTA = computed tomography angiography; NSTEMI = non-ST-segment elevation myocardial infarction; STEMI = ST-segment elevation myocardial infarction.

of 30-130 HU); low-attenuation plaque volume (LAPV) (plaque composition of -30 to 30 HU); and their normalized volume corresponding to the vessel, defined as the relevant plaque volume divided by the vessel volume, multiplied by 100 (percent TPV, percent NCPV, and percent LAPV).

CONVENTIONAL CORONARY CTA ANALYSIS. According to the standard coronary CTA interpretation criteria, Coronary Artery Disease Reporting and Data System (CAD-RADS) and APCs were obtained.[11] CAD-RADS is a standardized classification for stenosis severity ranging from 0 (ie, absence of plaque or stenosis) to 5 (ie, total occlusion).[11] APCs include low attenuation plaque (plaque with a pixel with ≤30 HU), positive remodeling (remodeling index of ≥1.1), spotty calcification (average density of >130 HU and diameter of <3 mm in any direction), and napkin ring sign (ring-like attenuation form with peripheral high and central lower attenuation portion). High-risk plaque (HRP) was defined as a lesion with ≥2 APCs.[11]

PRIMARY HYPOTHESIS AND ANALYSIS ENDPOINT. The working hypothesis of the study was that addition of the best quantitative plaque and hemodynamic features into the conventional coronary CTA analysis could enhance the discrimination ability for identification of the culprit lesions of ACS. The analysis endpoint was the differences in predictability between the reference model with CAD-RADS and HRP and the new prediction model that was constructed with the addition of the best AI-QCPHA features to the reference model. The best features were defined from the derivation cohort, and the model performance was compared between the new prediction model and the reference model in the validation cohort. A secondary analysis was performed using the model with only AI-QCPHA features.

STATISTICAL ANALYSIS. The detailed statistical methods are presented in the Supplemental Methods. In the selection of best features in the derivation cohort, hierarchical clustering was used to categorize similar features, and one feature from each cluster with the highest information gain for the culprit lesion was designated as an AI-QCPHA feature.[18] The prediction models were developed using the XGboost model,[19] which uses an ensemble of gradient-boosted decision trees and merges multiple weak classifiers (single-tier decision trees) into one robust classifier for predicting culprit lesions. Statistical significance was set at $P < 0.05$. All analyses were performed using R language version 4.2.0 (R Foundation for Statistical Computing). The R packages used in the current analysis are detailed in the Supplemental Methods.

RESULTS

BASELINE PATIENT CHARACTERISTICS. Among 449 enrolled ACS patients, 351 patients were finally

TABLE 2 Comparison of Lesion Characteristics Between Culprit and Nonculprit Lesions

	Derivation Cohort			Validation Cohort		
	Nonculprit Lesion (n = 1,247)	Culprit Lesion (n = 248)	*P* Value[a]	Nonculprit Lesion (n = 841)	Culprit Lesion (n = 115)	*P* Value[a]
Vessel			0.024			0.011
LAD	475 (38.1)	118 (47.6)		331 (39.4)	58 (50.4)	
LCX	312 (25.0)	53 (21.4)		220 (26.2)	30 (26.1)	
RCA	460 (36.9)	77 (31.0)		290 (34.5)	27 (23.5)	
CAD-RADS	1.0 (1.0-2.0)	3.0 (2.0-4.0)	<0.001	2.0 (1.0-3.0)	3.0 (2.0-4.0)	<0.001
0	19 (1.5)	0 (0.0)	<0.001	0 (0.0)	0 (0.0)	<0.001
1	624 (50.0)	37 (14.9)		335 (39.8)	12 (10.4)	
2	353 (28.3)	61 (24.6)		295 (35.1)	28 (24.3)	
3	161 (12.9)	81 (32.7)		148 (17.6)	25 (21.7)	
4	90 (7.2)	69 (27.8)		63 (7.5)	50 (43.5)	
APCs						
Low-attenuation plaque	146 (11.7)	101 (40.7)	<0.001	219 (26.0)	69 (60.0)	<0.001
Positive remodeling	256 (20.5)	116 (46.8)	<0.001	204 (24.3)	63 (54.8)	<0.001
Spotty calcification	82 (6.6)	55 (22.2)	<0.001	57 (6.8)	13 (11.3)	0.130
Napkin ring sign	33 (2.6)	30 (12.1)	<0.001	17 (2.0)	15 (13.0)	<0.001
High-risk plaque (≥2 APCs)	143 (11.5)	98 (39.5)	<0.001	192 (22.8)	64 (55.7)	<0.001
Quantitative plaque analysis						
Plaque burden, %	73.1 ± 15.0	85.2 ± 10.2	<0.001	71.9 ± 13.3	85.3 ± 11.3	<0.001
TPV, mm^3	79.9 ± 72.3	132.8 ± 96.9	<0.001	68.9 ± 67.7	119.2 ± 80.2	<0.001
NCPV, mm^3	70.1 ± 60.1	114.9 ± 82.4	<0.001	60.4 ± 56.6	107.4 ± 71.1	<0.001
LAPV, mm^3	2.2 ± 2.9	4.5 ± 5.1	<0.001	1.9 ± 3.6	4.4 ± 4.4	<0.001
Percent TPV	60.1 ± 14.5	69.3 ± 10.8	<0.001	59.7 ± 12.5	69.2 ± 11.0	<0.001
Percent NCPV	54.2 ± 13.1	61.5 ± 12.0	<0.001	53.8 ± 12.8	63.4 ± 12.0	<0.001
Percent LAPV	2.0 ± 2.3	2.8 ± 3.0	<0.001	1.9 ± 2.4	3.2 ± 3.7	<0.001
Quantitative hemodynamic analysis						
ΔFFR_{CT}	0.05 ± 0.08	0.16 ± 0.14	<0.001	0.04 ± 0.07	0.17 ± 0.15	<0.001
Peak FFR_{CT} gradient	0.02 ± 0.05	0.08 ± 0.09	<0.001	0.02 ± 0.04	0.08 ± 0.09	<0.001
Averaged WSS, $dyne/cm^2$	151.2 ± 103.0	229.8 ± 133.7	<0.001	141.1 ± 106.6	245.1 ± 179.2	<0.001
Peak WSS, $dyne/cm^2$	598.2 ± 861.4	1,550.1 ± 1,509.6	<0.001	502.5 ± 728.4	1,559.1 ± 1,517.8	<0.001
Averaged APS, $dyne/cm^2$	1,084.1 ± 1,970.8	1,671.6 ± 1,845.1	<0.001	2,098.1 ± 3,453.9	2,139.6 ± 2,338.9	0.880
Peak APS, $dyne/cm^2$	30,572.7 ± 15,631.5	39,968.8 ± 17,575.6	<0.001	29,521.9 ± 16,762.0	40,058.7 ± 16,576.5	<0.001
Averaged percent total MBF	22.6 ± 12.2	25.0 ± 9.6	<0.001	22.7 ± 12.4	26.4 ± 12.1	0.002
Peak percent total MBP	23.6 ± 13.1	27.2 ± 11.7	<0.001	23.8 ± 13.4	28.5 ± 14.0	0.001
Averaged percent left ventricular MBF	23.8 ± 13.7	26.9 ± 11.4	<0.001	24.1 ± 14.5	29.5 ± 14.7	<0.001
Peak percent left ventricular MBF	24.7 ± 14.8	29.3 ± 14.3	<0.001	25.2 ± 15.8	31.6 ± 17.0	<0.001

Values are n (%), mean ± SD, or median (Q1-Q3). [a]*P* values were derived from a generalized estimating equation model to account for the interrogated lesions within the same subjects.

APC = adverse plaque characteristics; APS = axial plaque stress; CAD-RADS = Coronary Artery Disease Reporting and Data System; FFR_{CT} = fractional flow reserve derived from coronary computed tomography angiography; LAD = left anterior descending artery; LAPV = low-attenuation plaque; LCX = left circumflex artery; MBF = myocardial blood flow; NCPV = noncalcified plaque volume; RCA = right coronary artery; TPV = total plaque volume; WSS = wall shear stress.

included in the study (Supplemental Figure 1) after exclusion of 47 (10.5%) patients with inadequate image quality for AI-QCPHA and 51 (11.4%) patients who had no identifiable culprit lesions; 243 patients and 108 patients were assigned to the derivation and validation cohorts, respectively. The baseline patient characteristics are presented in **Table 1**. The mean age of patients was 65.9 ± 11.7 years, and 74.4% of patients were male. The median time to event from coronary CTA to ACS was 375.0 (Q1-Q3: 95.0-644.5) days, and 223 patients (63.5%) presented with MI. Overall patient characteristics were well balanced between the derivation cohort and the validation cohort (**Table 1**).

COMPARISON OF LESION CHARACTERISTICS BETWEEN CULPRIT AND NONCULPRIT LESIONS. On coronary CTA, 1,495 lesions (248 [16.7%] culprit lesions) in the derivation cohort and 956 lesions (115 [12.0%] culprit lesions) in the validation cohort were identified. Coronary artery segments of culprit lesions are shown in Supplemental Table 2. CAD-RADS, APCs, and features from AI-QCPHA were compared between nonculprit and culprit lesions (**Table 2**). In the derivation

FIGURE 1 **Risk Stratification by CAD-RADS and HRP in the Derivation Cohort**

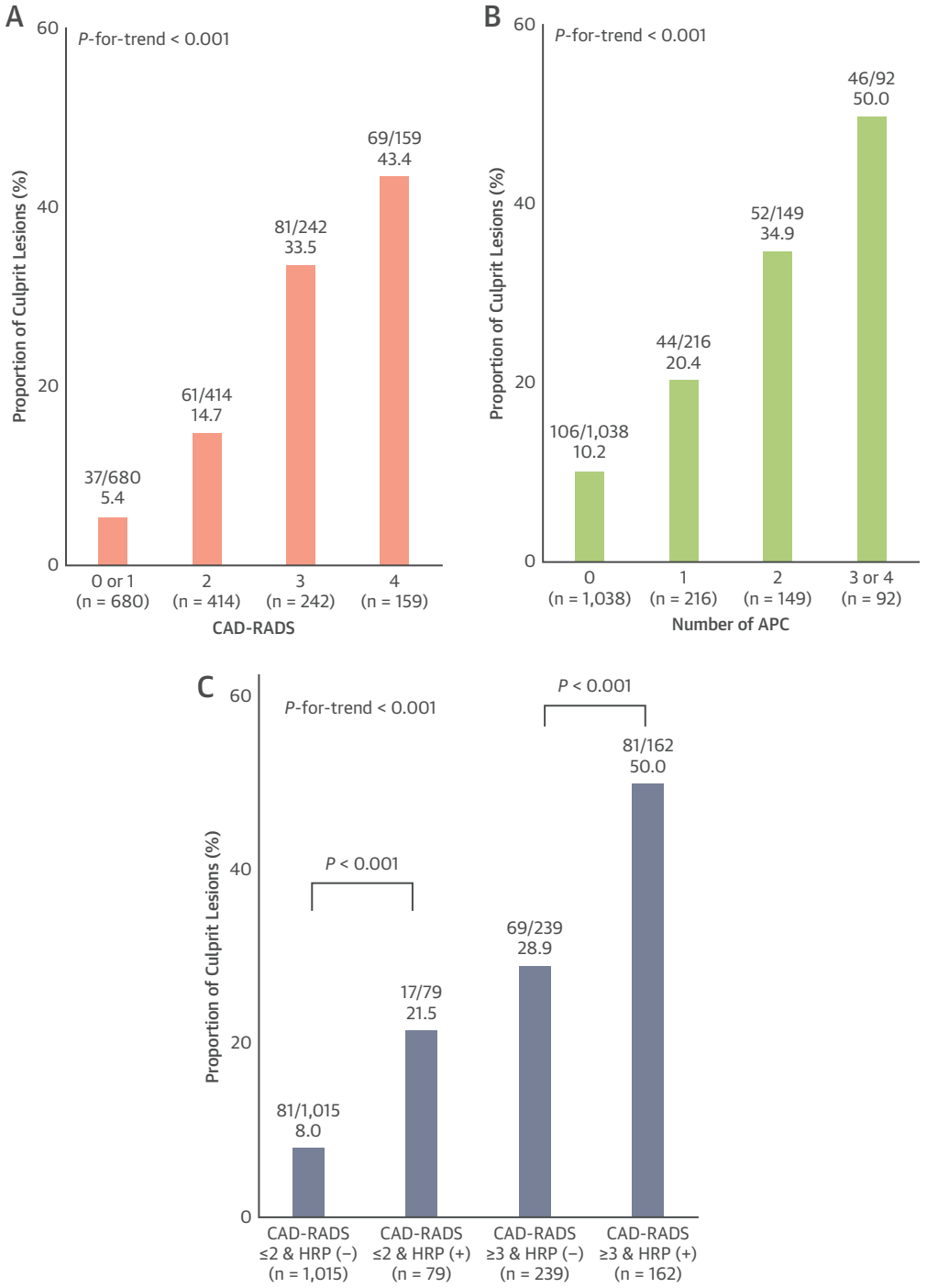

In the derivation cohort, the proportion of culprit lesions according to CAD-RADS (A), the number of APCs (B), and CAD-RADS of ≥3 and HRP (C) are shown. HRP was defined as the presence of ≥2 APCs. APCs included low-attenuation plaque, positive remodeling, spotty calcification, and napkin ring sign. APC = adverse plaque characteristic; CAD-RADS = Coronary Artery Disease Reporting and Data System; HRP = high-risk plaque.

JACC: CARDIOVASCULAR IMAGING, VOL. 17, NO. 9, 2024
SEPTEMBER 2024:1062–1076

FIGURE 2 Correlation and Relative Importance Among Plaque and Hemodynamic Features

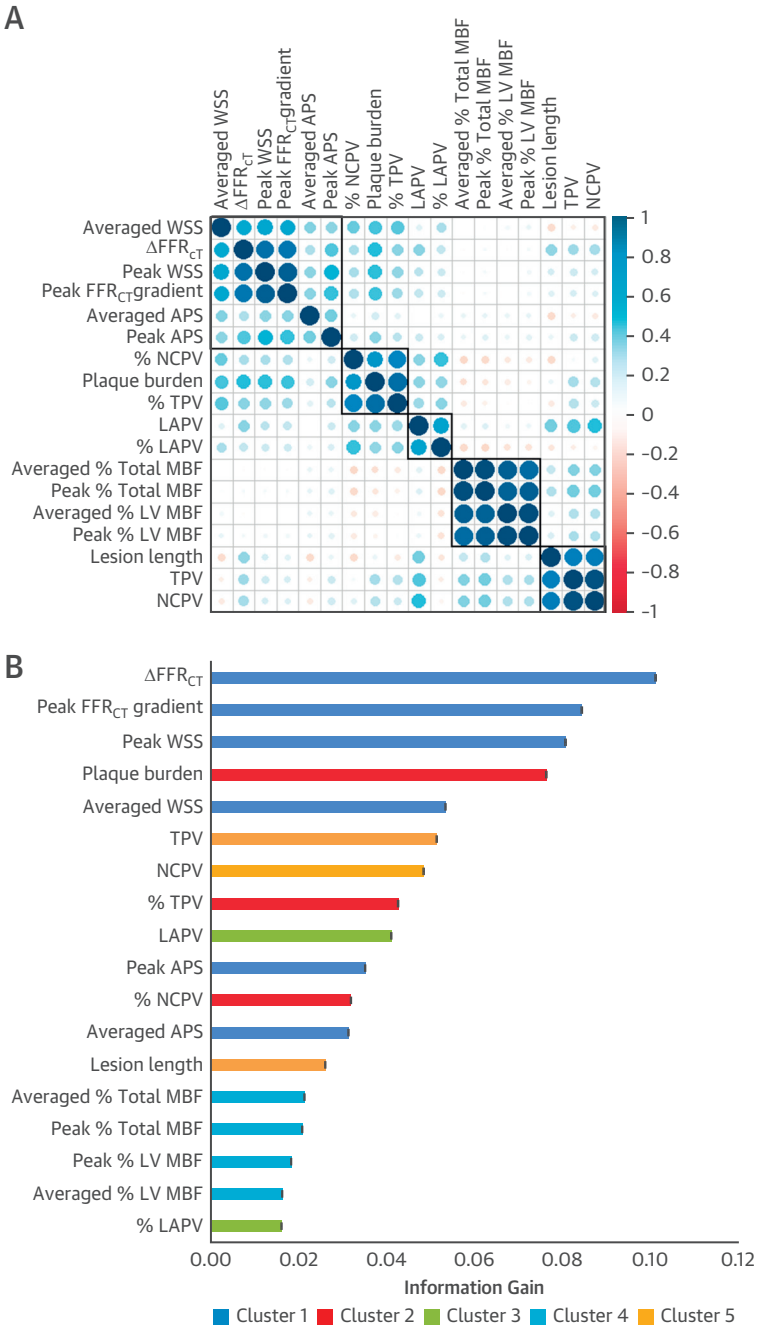

Eighteen features derived from AI-QCPHA were categorized into 5 clusters after hierarchical clustering (A), and the relative importance among them is presented according to the information gain criteria (B). The best features with the highest information gain within each cluster were ΔFFR_{CT}, plaque burden, TPV, LAPV, and averaged percent total MBF. AI-QCPHA = artificial intelligence-enabled quantitative coronary plaque and hemodynamic analysis; APS = axial plaque stress; FFR_{CT} = fractional flow reserve derived from coronary computed tomography angiography; LAPV = low-attenuation plaque volume; LV = left ventricular; MBF = myocardial blood flow; NCPV = noncalcified plaque volume; TPV = total plaque volume; WSS = wall shear stress.

FIGURE 3 **Incremental Value of AI-QCPHA Features Over CAD-RADS and HRP**

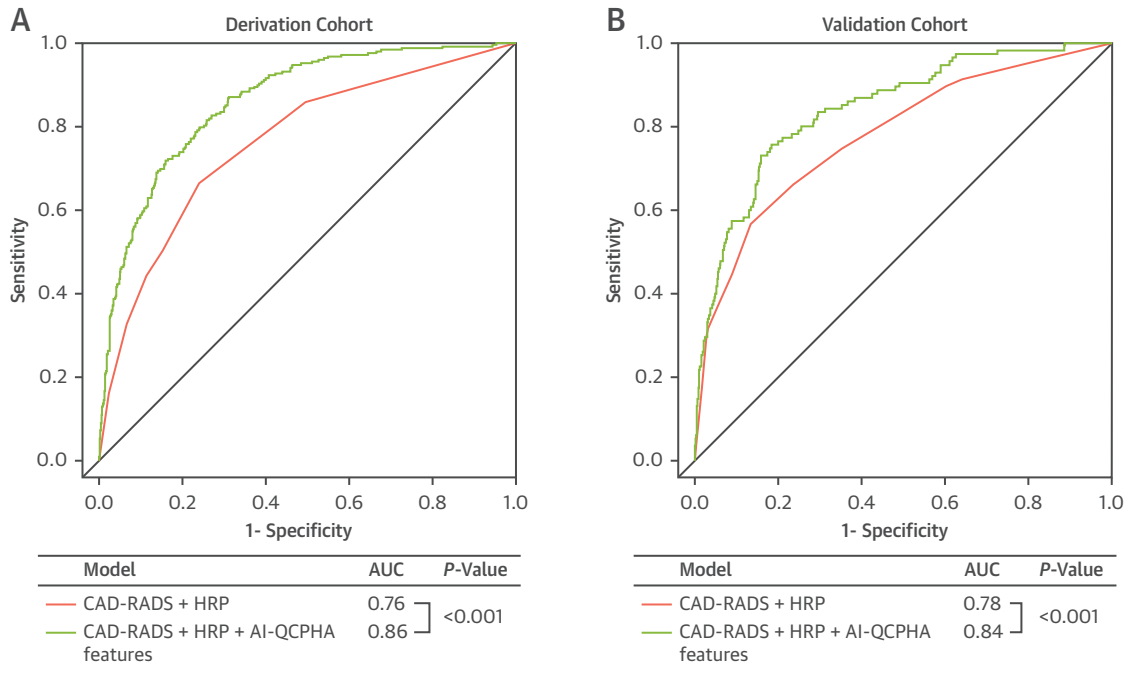

The predictability for culprit lesions of the model with CAD-RADS, HRP, and AI-QCPHA features was compared to that with CAD-RADS and HRP in the derivation cohort (A) and the validation cohort (B). HRP was defined as the presence of ≥2 APCs. AI-QCPHA features were ΔFFR_{CT}, plaque burden, total plaque volume, low-attenuation plaque volume, and averaged percent total myocardial blood flow. AUC = area under the curve; other abbreviations as in Figures 1 and 2.

cohort, culprit lesions had a higher CAD-RADS (3.0 [Q1-Q3: 2.0-4.0] vs 1.0 [Q1-Q3: 1.0-2.0]; $P < 0.001$) and a higher proportion of HRP (39.5% vs 11.5%; $P < 0.001$) compared to nonculprit lesions. In AI-QCPHA, culprit lesions showed a greater plaque burden, TPV, NCPV, LAPV, and normalized volume relative to the corresponding vessel volume (all $P < 0.001$). All hemodynamic parameters, including ΔFFR_{CT}, peak FFR_{CT} gradient, WSS, APS, percent total MBF, and percent left ventricular MBF, were also higher in culprit lesions compared to nonculprit lesions. These results were similar in the validation cohort (Table 2).

DISCRIMINATION FOR CULPRIT LESIONS BY THE CONVENTIONAL CORONARY CTA ANALYSIS. In the derivation cohort, the proportion of culprit lesions significantly increased with increasing CAD-RADS (5.4%, 14.7%, 33.%, and 43.4% for 0 or 1, 2, 3, and 4 in CAD-RADS, respectively; P for trend < 0.001) or the number of APCs (10.2%, 20.4%, 34.9%, and 50.0% for 0, 1, 2, and ≥3 APCs, respectively; P for trend < 0.001). The lesions with HRP showed a higher proportion of culprit lesions than those without HRP among lesions with CADS-RADS of ≤2 (21.5% vs 8.0; $P < 0.001$) or with CAD-RADS of ≥3 (50.0% vs 28.9%; $P < 0.001$) (Figure 1). Similar results were observed in the validation cohort (Supplemental Figure 2).

AI-QCPHA FEATURES AND THEIR INCREMENTAL VALUES TO CAD-RADS AND HRP. The covariance matrix of 18 features from AI-QCPHA in the derivation cohort is shown in Figure 2. Hierarchical clustering revealed 5 clusters, mainly representing hemodynamics, relative plaque burden, lipid-rich plaque volume, myocardial territory, and absolute amount of plaque. The best features from each cluster were ΔFFR_{CT}, plaque burden, TPV, LAPV, and averaged percent total MBF. These 5 AI-QCPHA features provided additive diagnostic performance for culprit lesions over CAD-RADS and HRP in the derivation cohort (AUC: 0.86 vs 0.76; $P < 0.001$). The additive value of 5 AI-QCPHA features was demonstrated in the validation cohort (AUC: 0.84 vs 0.78; $P < 0.001$) (Figure 3). In both the derivation and validation cohorts, all 5 AI-QCPHA features were associated with a higher risk of culprit lesions independent of CAD-RADS and APCs (Table 3). When each AI-QCPHA feature was added into the model with CAD-RADS

TABLE 3 Association of AI-QCPHA Features With ACS Culprit Lesions

	Unadjusted OR (95% CI)	*P* Value	Adjusted OR[a] (95% CI)	*P* Value
Derivation cohort				
ΔFFR_{CT}, per 0.1 increase	2.26 (1.96-2.60)	<0.001	1.68 (1.43-1.97)	<0.001
Plaque burden, per 10% increase	2.28 (1.96-2.67)	<0.001	1.62 (1.37-1.93)	<0.001
TPV, per 100-mm^3 increase	1.98 (1.71-2.29)	<0.001	1.48 (1.25-1.76)	<0.001
LAPV, per 10-mm^3 increase	4.49 (2.97-6.80)	<0.001	2.08 (1.38-3.14)	<0.001
Averaged percent total MBF, per 10% increase	1.17 (1.08-1.28)	<0.001	1.23 (1.10-1.37)	<0.001
Validation cohort				
ΔFFR_{CT}, per 0.1 increase	2.44 (1.95-3.05)	<0.001	1.83 (1.40-2.39)	<0.001
Plaque burden, per 10% increase	2.85 (2.15-3.77)	<0.001	2.01 (1.48-2.75)	<0.001
TPV, per 100-mm^3 increase	2.05 (1.59-2.65)	<0.001	1.75 (1.37-2.23)	<0.001
LAPV, per 10-mm^3 increase	3.56 (1.35-9.43)	0.011	2.03 (1.00-4.11)	0.049
Averaged percent total MBF, per 10% increase	1.24 (1.10-1.41)	<0.001	1.44 (1.21-1.70)	<0.001

APCs included low-attenuation plaque, positive remodeling, spotty calcification, and napkin-ring sign. HRP was defined as the presence of ≥2 APCs. [a]Adjusted for CAD-RADS and HRP.

AI-QCPHA = artificial intelligence–enabled coronary plaque and hemodynamic analysis; other abbreviations as in Tables 1 and 2.

and HRP in the reverse order of importance, the predictability of the models increased sequentially from 0.76 to 0.86 (Supplemental Figure 3). The incremental value of AI-QCPHA features was consistent when the reference model was defined as CAD-RADS, HRP, and FFR_{CT} (Supplemental Figure 4). The model with AI-QCPHA features showed a similar predictability to the new prediction model in both the derivation and validation cohorts (Supplemental Figure 5).

PROGNOSTIC IMPLICATIONS OF AI-QCPHA FEATURES BY THE TIME TO EVENT. In the entire cohort, 169 (48.1%) patients experienced ACS events within 1 year of coronary CTA, and 182 (51.9%) patients experienced ACS events after 1 year. When the relationship of the AI-QCPHA features with culprit risk was explored according to the time to event of 1 year, an increase in ΔFFR_{CT}, plaque burden, TPV, LAPV, and averaged percent total MBF was significantly associated with a higher risk of culprit lesion regardless of the time to event of 1 year (Table 4).

Figure 4 represents the time-dependent receiver-operating characteristic curve analysis according to 6-month intervals. When the predictabilities of the reference model (ie, CAD-RADS and HRP) and the new prediction model (ie, CAD-RADS, HRP, and AI-QCPHA features) were examined at different timepoints, the new prediction model consistently had a higher predictability than the reference model, regardless of the time to event, even though the overall predictability of both models tended to decrease in predicting long-term events. This result was consistent when the analysis was performed by the quartile of time intervals (Supplemental Figure 6).

INDIVIDUALIZED EXPLANATIONS OF THE RISK MODEL. The discriminatory gain of individual components of the new prediction model was assessed in SHAP (SHapley Additive exPlanations) waterfall plots (Supplemental Figure 7). Figure 5 depicts the representative case illustrating how each component of the new prediction model contributed to the classifier output when classifying a lesion as being a culprit or

TABLE 4 Relationship of AI-QCPHA Features With Short-Term and Long-Term ACS Risk

	Time-to-Event of >1 Year (n = 1,298)		Time-to-Event of ≤1 Year (n = 1,153)	
	Adjusted OR[a] (95% CI)	*P* Value	Adjusted OR[a] (95% CI)	*P* Value
ΔFFR_{CT}, per 0.1 increase	1.75 (1.44-2.11)	<0.001	1.79 (1.46-2.19)	<0.001
Plaque burden, per 10% increase	1.60 (1.31-1.95)	<0.001	2.20 (1.70-2.83)	<0.001
TPV, per 100-mm^3 increase	1.73 (1.44-2.08)	<0.001	1.47 (1.20-1.80)	<0.001
LAPV, per 10-mm^3 increase	2.09 (1.40-3.11)	<0.001	2.24 (1.12-4.48)	0.023
Averaged percent total MBF, per 10% increase	1.31 (1.16-1.48)	<0.001	1.30 (1.12-1.50)	<0.001

The definitions of HRP and AI-QCPHA features are the same as in Table 3. [a]Adjusted for CAD-RADS and HRP.

Abbreviations as in Tables 1 to 3.

nonculprit lesion. In the culprit lesion of the presented case, ΔFFR_{CT} provided the highest increment in classification output in the assessment of the lesion being an ACS culprit lesion (Figure 5A). When the event probability was plotted over time, the predicted time to event for a probability of ≥20%, which was the optimal threshold in predicting culprit lesions according to the Youden index (Supplemental Figure 8), was 384 days for this case, and the actual event time was 300 days.

DISCUSSION

The current study investigated the best predictors among AI-enabled coronary CTA-derived quantitative plaque and hemodynamic features in the prediction of ACS culprit lesions and their incremental prognostic value to the conventional coronary CTA analysis. The main findings were as follows. First, the probability of ACS culprit lesions increased with higher CAD-RADS and the presence of HRP, which is routinely used for coronary CTA reporting. Second, the best AI-QCPHA features were ΔFFR_{CT}, plaque burden, TPV, LAPV, and averaged percent total MBF, and they provided the additive predictive values for ACS culprit lesions over CAD-RADS and HRP in both the derivation and validation cohorts. The model with only AI-QCPHA features showed a similar performance to the new prediction model in both the derivation and validation cohorts. Third, the model with CAD-RADS, HRP, and AI-QCPHA showed higher predictability than the model with CAD-RAD and HRP, regardless of the time to event. Fourth, the explainable machine learning model identified ΔFFR_{CT} as the most impactful feature in the risk prediction model (Central Illustration).

RISK ASSESSMENT FOR ACS BASED ON CONVENTIONAL CORONARY CTA ANALYSIS. Coronary CTA is increasingly accepted as the first-line diagnostic modality for the assessment of CAD.[20] Using coronary CTA, it is possible to identify anatomic stenosis severity and plaque characteristics that correlate with coronary event risk,[20] and the ESC and ACC/AHA guideline recommends the use of coronary CTA for risk stratification in patients with CAD.[8,9] In the current study, we used CAD-RADS 2.0[11] assessed by independent radiologists as a reference model and found that stenosis severity and HRP based on visual estimation were associated with a higher risk of ACS; the prevalence of culprit lesions serially increased with higher CAD-RADS, and the presence of HRP further discriminated ACS culprit lesions within CAD-RADS of ≤2 and CAD-RADS of ≥3. This finding is in line with prior publications showing the relationship of CAD-RADS with short-term and long-term cardiovascular outcomes, including all-cause mortality or MI,[21,22] and the independent prognostic value of APC analysis on coronary CTA,[23] supporting the advantage of conventional coronary CTA analysis based on stenosis and plaque. In addition to visual analysis of coronary CTA, recent studies have suggested that additional coronary CTA parameters could further enhance the predictability for ACS risk. In ICONIC (Incident COroNary Syndromes Identified by Computed Tomography), quantitative fibrofatty or necrotic core volume was higher in ACS patients than in risk factor-matched control individuals,[4] and in the post hoc analysis of SCOT-HEART (Scottish COmputed Tomography of the HEART Trial), low-attenuation plaque burden of >4% was associated with more than 4-fold greater MI risk.[24] Similarly, in CAPIRE (Coronary Atherosclerosis in outlier subjects: Protective and novel Individual Risk factors Evaluation), LAPV, NCPV, and TPV provided additional predictive value for ACS events over clinical risk factors.[25] In the earlier EMERALD-I, the synergistic impact between local hemodynamic parameters and APCs on the risk for ACS development was reported.[14] The current evidence is consistent in showing the benefit of quantitative plaque analysis and

FIGURE 4 AUC Comparison According to the Time From Coronary CTA to ACS Events

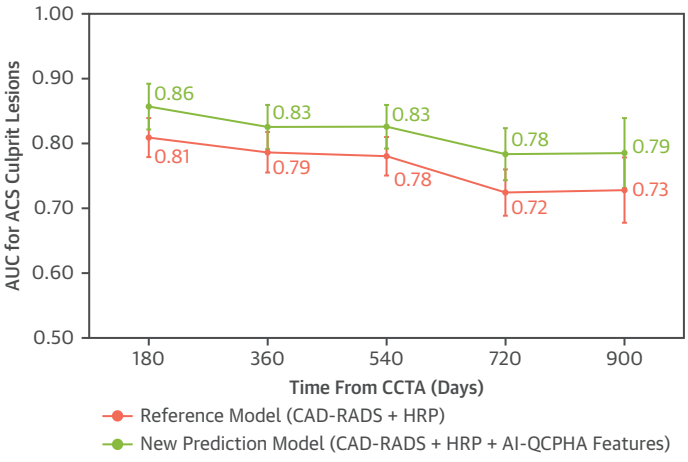

The AUCs for culprit lesions were compared between the reference model (ie, CAD-RADS and HRP) and the new prediction model (ie, CAD-RADS, HRP, and AI-QCPHA features) at different time intervals from coronary CTA. The error bars indicate 95% CIs. The definitions of HRP and AI-QCPHA features are the same as in Figure 3. CTA = computed tomography angiography; other abbreviations as in Figures 1 to 3.

FIGURE 5 Individual Risk Prediction With the Best AI-QCPHA Features

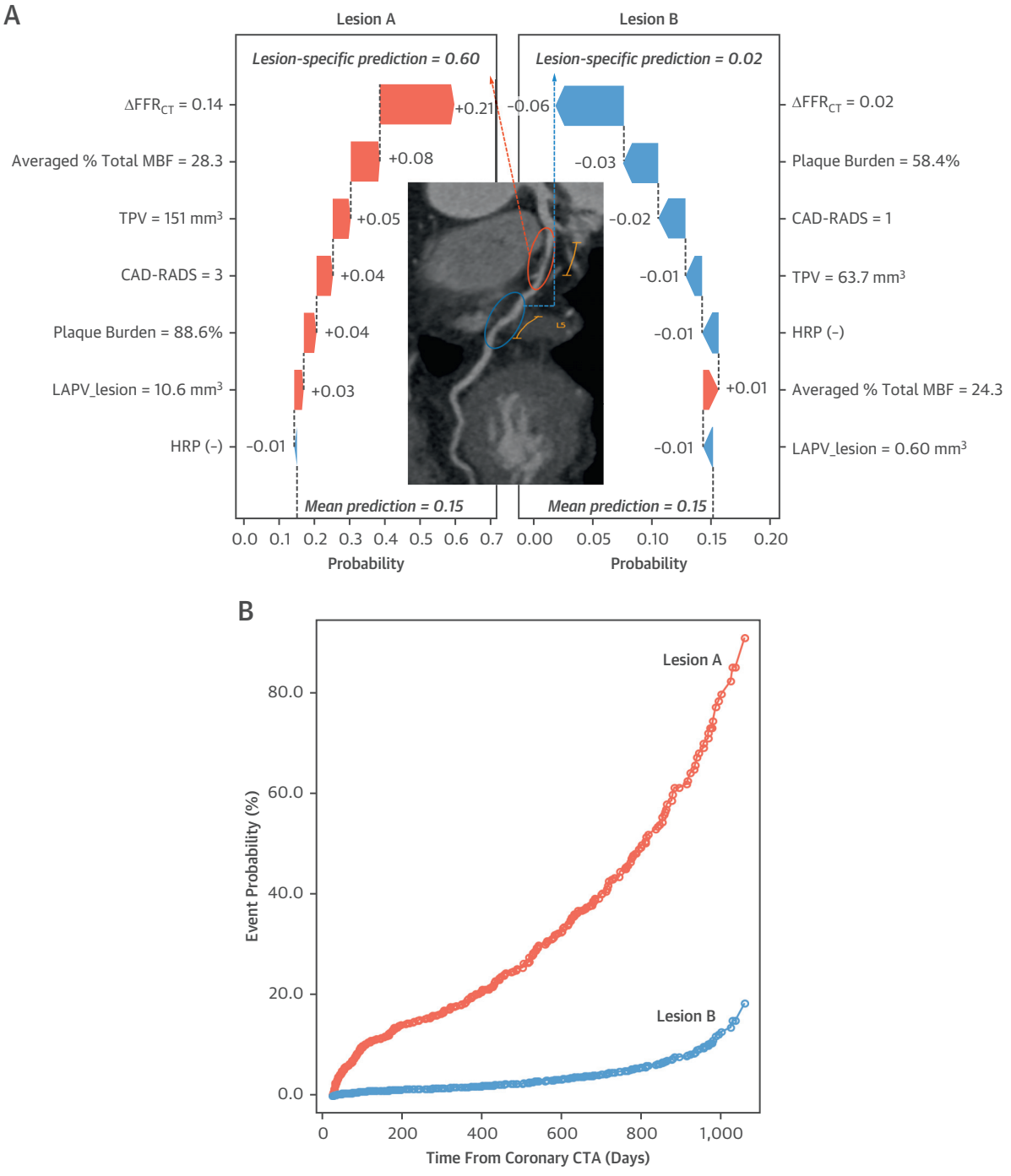

(A) In the waterfall plots for nonculprit and culprit lesions, Shapley additive explanations values of each component of the new prediction model (ie, CAD-RADS, HRP, and AI-QCPHA features) are shown with red arrows for increasing risk and blue arrows for decreasing risk of culprit lesions. (B) The event probability of nonculprit and culprit lesions is presented according to the time from coronary CTA. The definitions of HRP and AI-QCPHA features are the same as in Figure 3. Abbreviations as in Figures 1 to 4.

CENTRAL ILLUSTRATION **Identification of AI-QCPHA Features and Their Additive Value for Predicting ACS**

The EMERALD II Study

ACS Patients Who Underwent Coronary CTA From 1 Month to 3 Years Prior to ACS Event → Culprit vs Nonculprit Lesions in Coronary CTA

Derivation Cohort (1,495 Lesions)

AI-QCPHA

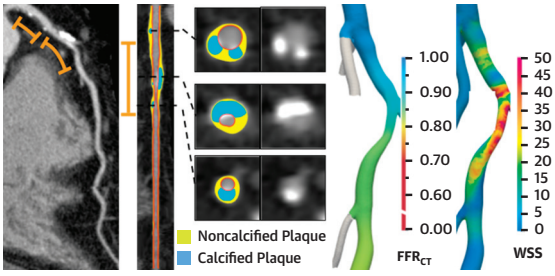

Features From AI-QCPHA

Plaque		Hemodynamics	
TPV, mm³	57	WSS (Avg), dyne/cm²	284
NCPV, mm³	34	WSS (Peak), dyne/cm²	743
LAPV, mm³	3.9	APS (Avg), dyne/cm²	588
% TPV	71	APS (Peak), dyne/cm²	28,099
% NCPV	43	ΔFFR$_{CT}$	0.10
% LAPV	5	Peak FFR$_{CT}$ gradient	0.02
Plaque burden, %	78	% Total MBF (Avg)	17
Lesion length, mm	13	% Total MBF (Peak)	30
		% LV MBF (Avg)	20
		% LV MBF (Peak)	36

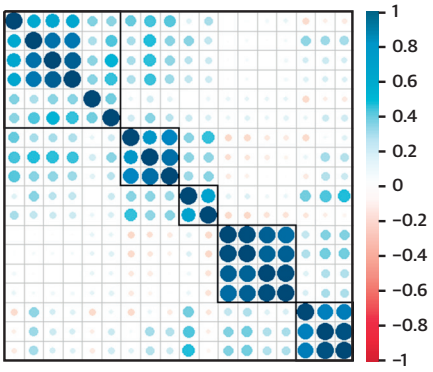

Hierarchical Clustering and Feature Selection

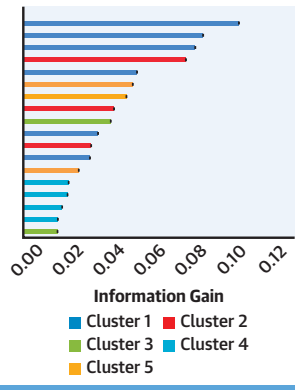

5 AI-QCPHA Features

ΔFFR$_{CT}$, plaque burden, total plaque volume, low-attenuation plaque volume, and averaged % total myocardial blood flow

Validation Cohort (956 Lesions)

Discrimination Ability for ACS Culprit Lesions

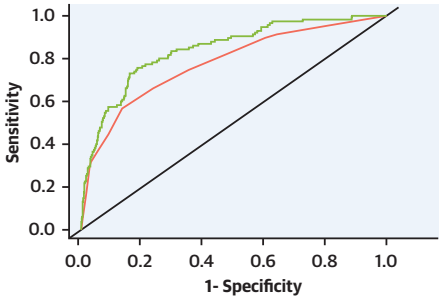

Model	AUC	*P* Value
CAD-RADS + HRP	0.78	<0.001
CAD-RADS + HRP + AI-QCPHA features	0.84	

Koo B-K, et al. JACC Cardiovasc Imaging. 2024;17(9):1062-1076.

Continued on the next page

hemodynamic assessment on coronary CTA for the prediction of future ACS, and the relative and combined prognostic value of these features, which have separately been proposed in prior studies, should be comprehensively validated in a reproducible manner. In this regard, EMERALD-II was designed to identify the best quantitative plaque and hemodynamic characteristics to predict ACS culprit lesions and to determine their prognostic values when added to the conventional coronary CTA analysis.

AI-ENABLED QUANTITATIVE CORONARY PLAQUE AND HEMODYNAMIC ASSESSMENT. Prior studies showing the potential benefits of plaque quantification and hemodynamic assessment on coronary CTA for risk stratification have mostly used semiautomated methods that need manual correction by experienced analyzers. Consequently, their routine clinical application is limited because of the additional required time and labor and variability among practitioners.[4,14,15,24-26] AI-based approaches for coronary CTA analysis are being used to resolve unmet needs for the clinical applicability of quantitative coronary CTA analysis.[17,27,28] In the current study, AI-QCPHA was developed to derive quantitative plaque and hemodynamic characteristics for generalizability, and data-driven feature selection methods were used to define the AI-QCPHA features to minimize the potential bias by analyzers.[18] Another strength of the current study is the prespecified derivation and validation cohorts at the upfront stage of the study, and AI-QCPHA for each cohort was independently performed, totally blinded to the information from the other cohort. Throughout this strict and thorough approach, 5 AI-QCPHA features were identified in the derivation cohort and demonstrated to significantly enhance the predictability for ACS risk of CAD-RADS and HRP in the validation cohort. This additive value was consistent even on top of CAD-RADS, HRP, and FFR_{CT}. An interesting finding is that the predictability was not different between the new prediction model with CAD-RADS, HRP, and AI-QCPHA features and the model with only AI-QCPHA features. Although this comparison should be further extrapolated in a large-scale study across various CAD severities, our findings indicate the potential benefit of AI-based coronary CTA quantitative analysis that can provide additional prognostic information.

IMPLICATIONS OF HRP AND HEMODYNAMIC CHARACTERISTICS FOR RISK STRATIFICATION AND TREATMENT STRATEGIES. In our study, the best AI-QCPHA features were ΔFFR_{CT}, plaque burden, TPV, LAPV, and averaged percent total MBF, and each feature contributed to the increment in the area under the curve in a stepwise manner over CAD-RADS and HRP. Given that these features represent local hemodynamics, relative and absolute atherosclerotic burden, lipid-rich plaque, and subtended myocardial territory, our findings support the pathophysiology of ACS events[13,29] and demonstrate the incremental prognostic value of integrating each coronary CTA-defined attribute proven in prior studies.[4,14,15,24,25] These findings align with the post hoc analysis of ICONIC, showing the better predictability of the machine learning model derived by applying a boosted ensemble algorithm to quantitative plaque features than the models with percent diameter stenosis or HRP. It is important to highlight that in the current study, the incidence of ST-segment elevation MI was higher compared to what was observed in ICONIC. This discrepancy may be attributable to the fact that the East Asian population, which constituted about two-thirds of the study population, tends to exhibit a higher incidence of ST-segment elevation MI.[30,31] Of note, the incremental predictability of 5 AI-QCPHA features was maintained across different timepoints from coronary CTA, and the explainable machine learning models implied that ΔFFR_{CT} provided the highest impact on the increment in ACS risk among the model components. Therefore, in addition to the

CENTRAL ILLUSTRATION Continued

In EMERALD II, which enrolled ACS patients who underwent coronary computed tomography angiography from 1 month to 3 years before the ACS event, coronary plaque and hemodynamic lesion features on coronary CTA were contrasted between culprit and nonculprit lesions. AI-QCPHA was performed, and ΔFFR_{CT}, plaque burden, total plaque volume, low-attenuation plaque volume, and averaged percent total myocardial blood flow were identified as the best features. In the validation cohort, the addition of AI-QCPHA features to CAD-RADS and HRP significantly enhanced the ability to discriminate culprit lesions from nonculprit lesions. HRP was defined as the presence of ≥2 APCs. APCs included low-attenuation plaque, positive remodeling, spotty calcification, and napkin-ring sign. ACS = acute coronary syndrome; AI-QCPHA = artificial intelligence-enabled quantitative coronary plaque and hemodynamic analysis; APC = adverse plaque characteristic; APS = axial plaque stress; AUC = area under the curve; Avg = average; CAD-RADS = Coronary Artery Disease Reporting and Data System; CTA = computed tomography angiography; EMERALD-II = Exploring the Mechanism of Plaque Rupture in Acute Coronary Syndrome Using Coronary Computed Tomography Angiography and Computational Fluid Dynamics II; FFR_{CT} = fractional flow reserve derived from coronary computed tomography angiography; HRP = high-risk plaque; LAPV = low-attenuation plaque volume; MBF = myocardial blood flow; NCPV = noncalcified plaque volume; TPV = total plaque volume; WSS = wall shear stress.

prior published reports, EMERALD-II further highlights the importance of incorporating a broader domain of CAD, including physiologic and myocardial territory assessments as well as quantitative plaque features, in defining the ACS risk. This study also showed the clinical applicability of integrative AI-QCPHA that could enable physicians to define target lesions at greater risk of ACS events and might overcome the limitations of low positive predictive value solely based on anatomic or plaque features.[12,32] Further investigation is required to assess the effectiveness of prevention strategies with optimal medical therapy or percutaneous coronary intervention for high-risk lesions based on our risk model.

STUDY LIMITATIONS. The current study has several limitations. First, the data were collected in a retrospective way among ACS patients. Nonetheless, the sample size was based on the prespecified assumption, with each derivation and validation cohort meeting the criteria set forth in the sample size calculation. The primary hypothesis was met with an appropriate study population. Second, the control group was set as internal controls, which were nonculprit lesions within patients. The risk model should be validated by comparing culprit lesions with external controls of patients without ACS in future studies. Third, although the risk model derived from the derivation cohort was validated in the independent validation cohort, there was no external cohort, which warrants extrapolation of the current results in other populations. Fourth, the patient-level factors between coronary CTA and ACS events, including glucose and lipid profiles, lifestyle modification, and medication history, were not included in the study. However, the study design using internal controls might have reduced the effect of the patient-level factors on the current results. Fifth, the current analysis was not tested according to CT technology and needs to be validated across various CT technologies.

CONCLUSIONS

AI-QCPHA has the potential to enhance the prediction of lesion-specific ACS risk when added to conventional coronary CTA analysis. The use and integration of such algorithms in clinical practice can provide an improved risk stratification with the aim of preventing ACS and for the optimization of treatment strategy for patients with CAD.

FUNDING SUPPORT AND AUTHOR DISCLOSURES

This study received funding from HeartFlow Inc. The company performed the computational fluid dynamics, and artificial intelligence quantitative coronary plaque analysis but was not involved in the study design, collection, analysis, and interpretation of data; the writing of this paper; or the decision to submit it for publication. Dr Koo has received institutional research grants from Abbott, Philips, and HeartFlow Inc. Dr Nam has received institutional research grants from Abbott and Genoss. Dr Merkely has received direct personal payments for speaker fees or studies from Abbott, AstraZeneca, Biotronik, Boehringer Ingelheim, CSL Behring, Daiichi Sankyo, DUKE Clinical Institute, Medtronic, and Novartis and institutional grants from Abbott, AstraZeneca, Biotronik, Boehringer Ingelheim, Boston Scientific, Bristol Myers Squibb, CSL Behring, Daiichi Sankyo, DUKE Clinical Institute, Eli Lilly, Medtronic, Novartis, Terumo, and VIFOR Pharma. Dr de Bruyne has received institutional unrestricted research grants from Abbott, Boston Scientific, and Biotronik; has received consulting fees from Abbott, Opsens, and Boston Scientific; and is a shareholder for Siemens, GE, Bayer, Philips, HeartFlow Inc, Edwards Life Sciences, Sanofi, and Omega Pharma. Dr Ko has equity in Artrya and has received honoraria from Medtronic, Abbott Vascular, and Canon Medical. Dr Leipsic is a consultant for and holds stock options in HeartFlow Inc and modest personal core lab fees from Arineta. Dr Shah has received honoraria as a speaker for HeartFlow Inc. Dr Bax has received unrestricted research grants from Abbott and Edwards Lifesciences to the Department of Cardiology, Leiden University Medical Center, the Netherlands. Dr Shaw has received honoraria from HeartFlow Inc and Elucid Imaging. All other authors have reported that they have no relationships relevant to the contents of this paper to disclose.

ADDRESS FOR CORRESPONDENCE: Dr Bon-Kwon Koo, Division of Cardiology, Department of Internal Medicine, Seoul National University Hospital, 101 Daehang-ro, Chongno-gu, Seoul 03080, Korea. E-mail: bkkoo@snu.ac.kr.

PERSPECTIVES

COMPETENCY IN PATIENT CARE AND PROCEDURAL SKILLS: With the use of AI-QCPHA on coronary CTA, quantitative and qualitative plaque characteristics, local hemodynamics, and myocardial territory were comprehensively assessed, and 5 AI-QCPHA features provided incremental predictability for ACS risk over the conventional coronary CTA analysis.

TRANSLATIONAL OUTLOOK: Future studies are needed to investigate the efficacy of prevention strategies based on AI-QCPHA.

REFERENCES

1. Ruff CT, Braunwald E. The evolving epidemiology of acute coronary syndromes. *Nat Rev Cardiol*. 2011;8:140–147. https://doi.org/10.1038/nrcardio.2010.199

2. Bergmark BA, Mathenge N, Merlini PA, Lawrence-Wright MB, Giugliano RP. Acute coronary syndromes. *Lancet*. 2022;399:1347–1358. https://doi.org/10.1016/S0140-6736(21)02391-6

3. Virani SS, Alonso A, Aparicio HJ, et al. Heart disease and stroke statistics—2021 update: a report from the American Heart Association. *Circulation*. 2021;143:e254–e743. https://doi.org/10.1161/CIR.0000000000000950

4. Chang HJ, Lin FY, Lee SE, et al. Coronary atherosclerotic precursors of acute coronary syndromes. *J Am Coll Cardiol*. 2018;71:2511–2522. https://doi.org/10.1016/j.jacc.2018.02.079

5. Maddox TM, Stanislawski MA, Grunwald GK, et al. Nonobstructive coronary artery disease and risk of myocardial infarction. *JAMA*. 2014;312:1754–1763. https://doi.org/10.1001/jama.2014.14681

6. Investigators S-H, Newby DE, Adamson PD, et al. Coronary CT angiography and 5-year risk of myocardial infarction. *N Engl J Med*. 2018;379:924–933. https://doi.org/10.1056/NEJMoa1805971

7. Douglas PS, Hoffmann U, Patel MR, et al. Outcomes of anatomical versus functional testing for coronary artery disease. *N Engl J Med*. 2015;372:1291–1300. https://doi.org/10.1056/NEJMoa1415516

8. Knuuti J, Wijns W, Saraste A, et al. 2019 ESC guidelines for the diagnosis and management of chronic coronary syndromes. *Eur Heart J*. 2020;41:407–477. https://doi.org/10.1093/eurheartj/ehz425

9. Gulati M, Levy PD, Mukherjee D, et al. 2021 AHA/ACC/ASE/CHEST/SAEM/SCCT/SCMR guideline for the evaluation and diagnosis of chest pain: a report of the American College of Cardiology/American Heart Association Joint Committee on Clinical Practice Guidelines. *J Am Coll Cardiol*. 2021;78(22):2218–2261. https://www.jacc.org/doi/10.1016/j.jacc.2021.07.052

10. Maurovich-Horvat P, Ferencik M, Voros S, Merkely B, Hoffmann U. Comprehensive plaque assessment by coronary CT angiography. *Nat Rev Cardiol*. 2014;11:390–402. https://doi.org/10.1038/nrcardio.2014.60

11. Cury RC, Leipsic J, Abbara S, et al. CAD-RADS 2.0—2022 Coronary Artery Disease-Reporting and Data System: an expert consensus document of the Society of Cardiovascular Computed Tomography (SCCT), the American College of Cardiology (ACC), the American College of Radiology (ACR), and the North America Society of Cardiovascular Imaging (NASCI). *JACC Cardiovasc Imaging*. 2022;15:1974–2001. https://doi.org/10.1016/j.jcmg.2022.07.002

12. Kaul S, Narula J. In search of the vulnerable plaque: is there any light at the end of the catheter? *J Am Coll Cardiol*. 2014;64:2519–2524. https://doi.org/10.1016/j.jacc.2014.10.017

13. Yang S, Koo BK, Narula J. Interactions between morphological plaque characteristics and coronary physiology: from pathophysiological basis to clinical implications. *JACC Cardiovasc Imaging*. 2022;15:1139–1151. https://doi.org/10.1016/j.jcmg.2021.10.009

14. Lee JM, Choi G, Koo BK, et al. Identification of high-risk plaques destined to cause acute coronary syndrome using coronary computed tomographic angiography and computational fluid dynamics. *JACC Cardiovasc Imaging*. 2019;12:1032–1043. https://doi.org/10.1016/j.jcmg.2018.01.023

15. Lee SH, Hong D, Dai N, et al. Anatomic and hemodynamic plaque characteristics for subsequent coronary events. *Front Cardiovasc Med*. 2022;9:871450. https://doi.org/10.3389/fcvm.2022.871450

16. Thygesen K, Alpert JS, Jaffe AS, et al. Fourth universal definition of myocardial infarction (2018). *Eur Heart J*. 2019;40:237–269. https://doi.org/10.1093/eurheartj/ehy462

17. Tzimas G, Gulsin GS, Everett RJ, et al. Age- and sex-specific nomographic CT quantitative plaque data from a large international cohort. *JACC Cardiovasc Imaging*. 2024;17(2):165–175. https://doi.org/10.1016/j.jcmg.2023.05.011

18. Yang S, Koo BK, Hoshino M, et al. CT angiographic and plaque predictors of functionally significant coronary disease and outcome using machine learning. *JACC Cardiovasc Imaging*. 2021;14:629–641. https://doi.org/10.1016/j.jcmg.2020.08.025

19. Al'Aref SJ, Singh G, Choi JW, et al. A boosted ensemble algorithm for determination of plaque stability in high-risk patients on coronary CTA. *JACC Cardiovasc Imaging*. 2020;13:2162–2173. https://doi.org/10.1016/j.jcmg.2020.03.025

20. Serruys PW, Hara H, Garg S, et al. Coronary computed tomographic angiography for complete assessment of coronary artery disease: *JACC* state-of-the-art review. *J Am Coll Cardiol*. 2021;78:713–736. https://doi.org/10.1016/j.jacc.2021.06.019

21. Xie JX, Cury RC, Leipsic J, et al. The Coronary Artery Disease-Reporting and Data System (CAD-RADS): prognostic and clinical implications associated with standardized coronary computed tomography angiography reporting. *JACC Cardiovasc Imaging*. 2018;11:78–89. https://doi.org/10.1016/j.jcmg.2017.08.026

22. Bittner DO, Mayrhofer T, Budoff M, et al. Prognostic value of coronary CTA in stable chest pain: CAD-RADS, CAC, and cardiovascular events in PROMISE. *JACC Cardiovasc Imaging*. 2020;13:1534–1545. https://doi.org/10.1016/j.jcmg.2019.09.012

23. Yang S, Hoshino M, Koo BK, et al. Relationship of plaque features at coronary CT to coronary hemodynamics and cardiovascular events. *Radiology*. 2022;305:578–587. https://doi.org/10.1148/radiol.213271

24. Williams MC, Kwiecinski J, Doris M, et al. Low-attenuation noncalcified plaque on coronary computed tomography angiography predicts myocardial infarction: results from the multicenter SCOT-HEART Trial (Scottish Computed Tomography of the HEART). *Circulation*. 2020;141:1452–1462. https://doi.org/10.1161/CIRCULATIONAHA.119.044720

25. Andreini D, Magnoni M, Conte E, et al. Coronary plaque features on CTA can identify patients at increased risk of cardiovascular events. *JACC Cardiovasc Imaging*. 2020;13:1704–1717. https://doi.org/10.1016/j.jcmg.2019.06.019

26. Yang S, Lee JM, Hoshino M, et al. Prognostic implications of comprehensive whole vessel plaque quantification using coronary computed tomography angiography. *JACC Asia*. 2021;1:37–48. https://doi.org/10.1016/j.jacasi.2021.05.003

27. Griffin WF, Choi AD, Riess JS, et al. AI evaluation of stenosis on coronary CT angiography, comparison with quantitative coronary angiography and fractional flow reserve: a CREDENCE Trial substudy. *JACC Cardiovasc Imaging*. 2023;16(2):193–205. https://doi.org/10.1016/j.jcmg.2021.10.020

28. Nurmohamed NS, Bom MJ, Jukema RA, et al. AI-guided quantitative plaque staging predicts long-term cardiovascular outcomes in patients at risk for atherosclerotic CVD. *JACC Cardiovasc Imaging*. 2024;17(3):269–280. https://doi.org/10.1016/j.jcmg.2023.05.020

29. Ford TJ, Berry C, De Bruyne B, et al. Physiological predictors of acute coronary syndromes: emerging insights from the plaque to the vulnerable patient. *JACC Cardiovasc Interv*. 2017;10:2539–2547. https://doi.org/10.1016/j.jcin.2017.08.059

30. Sim DS, Jeong MH. Differences in the Korea Acute Myocardial Infarction Registry compared with Western registries. *Korean Circ J*. 2017;47:811–822. https://doi.org/10.4070/kcj.2017.0027

31. Inohara T, Kohsaka S, Spertus JA, et al. Comparative trends in percutaneous coronary intervention in Japan and the United States, 2013 to 2017. *J Am Coll Cardiol*. 2020;76:1328–1340. https://doi.org/10.1016/j.jacc.2020.07.037

32. Kumar A, Thompson EW, Lefieux A, et al. High coronary shear stress in patients with coronary artery disease predicts myocardial infarction. *J Am Coll Cardiol*. 2018;72:1926–1935. https://doi.org/10.1016/j.jacc.2018.07.075

KEY WORDS acute coronary syndrome, artificial intelligence, coronary CT angiography, hemodynamics, plaque characteristics

APPENDIX For an expanded Methods section as well as supplemental figures, tables, and references, please see the online version of this paper.